

Photovoltaics from soluble small molecules

Solution-processable small molecules have attractive features for application in photovoltaic cells. They offer the facile processing associated with polymers, yet are easier to synthesize and purify, are monodisperse, and typically show higher charge carrier mobilities. Recent progress in solution-processable small molecule blends has yielded photovoltaic cells with efficiencies exceeding 1%. This article reviews progress in this nascent field and discusses the requirements imposed by the need for charge separation within an interpenetrating network, energy level tuning for light absorption and voltage output, and processing techniques to achieve phase separation on excitonic length scales. Design criteria for next-generation materials are provided.

Matthew T. Lloyd¹, John E. Anthony², and George G. Malliaras^{1,*}

¹Department of Materials Science and Engineering, Cornell University, Ithaca, New York, 14853, USA

²Department of Chemistry, University of Kentucky, Lexington, Kentucky, 40506, USA

*E-mail: ggm1@cornell.edu

The first bilayer device that established the field of organic photovoltaics (OPV) was devised by Tang¹ in 1986. The Tang cell consisted of donor and acceptor layers deposited by sequential thermal vacuum sublimation of two small molecules. From these early devices it was determined that, unlike an inorganic photovoltaic device, efficient operation in an organic cell requires two semiconducting materials with a band-edge offset to split photogenerated electron/hole pairs² efficiently. The second breakthrough was made ten years later, when the first bulk heterojunction solar cell was realized^{3,4}. This design allows for extraction of charges from a much larger volume of active material, increasing both light absorption and photocurrent

generation. Today, research focuses on controlling donor/acceptor (D/A) phase separation, increasing and balancing charge-carrier mobilities, and searching for materials that maximally absorb the solar spectrum without sacrificing photovoltage.

Small molecules are known to have among the highest charge-carrier mobilities for organic semiconductors, with values as high as 15 cm²/V.s measured in single-crystal rubrene field-effect transistors⁵. Vacuum thermal gradient sublimation of low molecular weight molecules permits high levels of purification⁶. They are monodisperse, and parameters such as regioregularity and polydispersity are not an issue. Finally, the synthesis of small molecules is usually simpler relative to polymeric semiconductors. These attributes and the performance

of early-stage devices show the potential for soluble small molecules to be low temperature solution-processed systems for realizing phase-separated networks with easily tunable energy levels.

This review covers the use of soluble small molecules as the active materials in OPV cells. Advancement of this new class of materials for photovoltaic devices benefits extensively from progress in vacuum-deposited small molecules, as well as polymeric semiconductors. The well-established, and higher performing, polymeric semiconductor systems are covered here only briefly, and the reader is referred elsewhere for greater depth and scope.

Photovoltaic mechanism

Incident photons can be absorbed by either the hole-transporting (donor) or the electron-transporting (acceptor) material. Compared with inorganic semiconductors, the dielectric constant in organic materials is low ($\epsilon \sim 3\text{--}4$). Consequently, photoinduced excited states result in coulombically bound electron-hole (e^-/h^+) pairs with a binding energy⁷ of 0.4–1.4 eV. This neutral particle, referred to as an exciton, participates in random-walk diffusion (Fig. 1).

Excitons can be dissociated into polarons (weakly localized charge carriers) at the D/A heterojunction. The energy level offset between the molecular orbitals of the donor and acceptor layers provides the driving force for elementary charge transfer (Fig. 1a, process 1). For example, when the lowest unoccupied molecular orbital (LUMO) energy difference is greater than the exciton binding energy, subpicosecond charge transfer takes place from the donor to the acceptor^{8,9}. Excitons within the acceptor layer are similarly dissociated by hole transfer between the highest occupied molecular orbitals (HOMOs) at the heterojunction. Charge recombination pathways also exist. However, recombination rate constants in efficient heterojunctions are typically at least an order of magnitude slower than those for charge separation, giving rise to persistent, long-lived ionized states^{4,10}.

Preceding charge separation, an energy transfer step may occur. In this case, photoexcited exciton transfer from the donor to the acceptor is followed by hole injection back to the donor (Fig. 1a, process 2)¹¹. While a two-step exciton dissociation pathway does not necessarily hinder the function of most organic solar cells¹², it places a lower limit on the size of the donor bandgap (E_{gap}).

Device design

Light absorption

The maximum photon flux of the solar spectrum (at 1.6–1.8 eV) lies slightly beyond the reach of most organic semiconductors, which have bandgaps^{13,14} >1.8 eV. For single E_{gap} solar cells, an E_{gap} of 1.4 eV optimally absorbs the solar spectrum with a maximum theoretical power conversion efficiency¹⁵ of 31%. For organic heterojunctions comprised of two semiconductors, like high-performance inorganic multijunction solar cells, the potential absorption cross section can be extended beyond that of a single E_{gap} cell¹⁶.

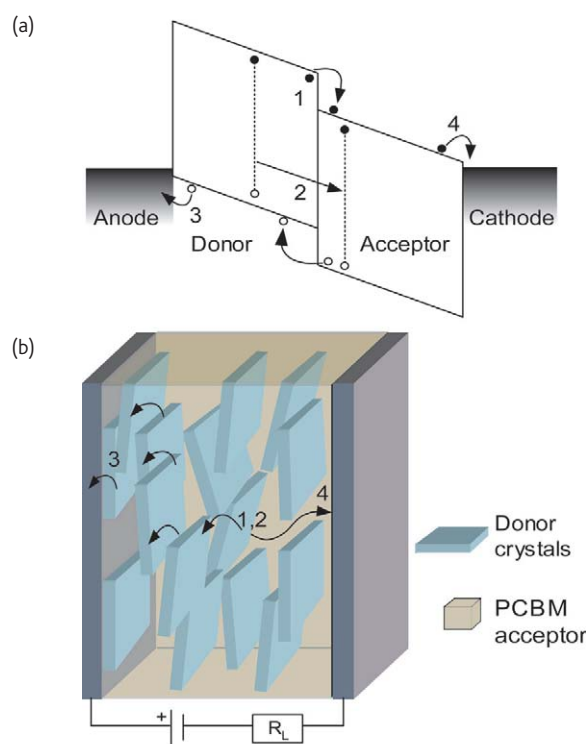


Fig. 1 (a) Energy level diagram for a D/A heterojunction under short-circuit conditions. (1) Photoexcited excitons diffuse to a D/A interface followed by electron transfer to the LUMO of the acceptor. (2) In some cases, a two-step process may occur where charge transfer is preceded by an energy transfer event. (b) Schematic of a device fabricated from a crystalline donor material such as the ones reviewed here. After dissociation (1,2), holes traverse one or more crystalline donor domains for charge collection at the anode (3). Meanwhile, the amorphous PCBM acceptor material excluded from the crystalline domains of the small molecules forms a continuous network for electron transport to the cathode (4).

A great deal of work has been carried out to successfully harvest the longer wavelengths of the solar spectrum using synthetic routes to decrease the bandgap of the absorbing layers^{17–20}. This has yielded new materials that absorb to at least 1.6 eV and exhibit a high molar extinction coefficient throughout the visible¹⁴. Absorption can also be enhanced by doping one of the layers with a material that absorbs light where the others do not. Excitons from high-energy photons absorbed by the dopant may transfer to the other layers, eliminating 'dips' in the absorption spectrum and producing a uniform spectral response.

Charge carrier mobility

Semiconductors with high mobility will extract charge from the D/A interface more rapidly, reducing steady-state charge buildup. The result is a low density of interfacial charge carriers that decreases recombination rates and is thought to increase device performance. Material defects and impurities tend to degrade carrier mobility in organic semiconductors. Salzman *et al.*²¹ investigated the effect of impurities in OPV devices fabricated from vacuum-deposited copper phthalocyanine (CuPc). Power conversion efficiency increases five-fold

after purification of the CuPc by various thermal vacuum sublimation techniques. The increase was attributed to a 10^3 enhancement in hole mobility after the elimination of metal-free phthalocyanine.

Despite trends such as these, and the intuition that higher mobility leads to higher performance, recent work carried out by Mandoc *et al.*²² suggests that excessively high mobilities can be detrimental to some device parameters. According to calculations, materials with a mobility of $1 \times 10^{-5} \text{ cm}^2/\text{V.s}$ achieve an exciton dissociation probability close to 100%. Any additional increase in the mobility reduces charge accumulation within the device, effectively shifting the quasi-Fermi levels of the donor and acceptor. This shift in D/A energy levels reduces the open-circuit voltage (V_{oc}) and decreases the overall device efficiency. For one-sun illumination (solar intensity at the Earth's surface, $\sim 100 \text{ mW}/\text{cm}^2$), calculations predict an optimum mobility between 10^{-6} – $10^{-5} \text{ cm}^2/\text{V.s}$, while higher mobilities are only required for higher photon fluxes associated with concentrated sunlight.

The ratio of the donor and acceptor charge-carrier mobilities also influences device performance, the extent of which is still under debate. A study of recombination in polymer/fullerene cells by Koster *et al.*²³ demonstrated that the rate of recombination is dominated by the lower mobility material. The recombination rate directly affects the device fill factor (squareness of the I – V curve), and ultimately device efficiency. Both model and experimental data suggest that values for the fill factors are highest when the h^+/e^- mobility ratio approaches unity. Another view is offered by Peumans *et al.*²⁴, who measured the effect of mobility mismatch on the probability of exciton dissociation. In this context, the likelihood for a given h^+/e^- pair to remain separated decreases as the mobility ratio approaches unity.

Since efficient operation of OPVs depends on the diffusion of excitons to a charge-separating interface, materials that sustain long exciton lifetimes are a design target. Exciton diffusion lengths are usually correlated to high charge-carrier mobility^{25,26}. High exciton diffusion lengths also translate to coarser (and more easily fabricated) phase-separated networks in bulk heterojunctions, and thicker, more absorbing, layered device architectures. Increasing material purity and crystallinity are two ways to increase exciton diffusion lengths^{27,28}.

Frontier orbital energy levels

As discussed earlier, the D/A band-edges must be offset by a value that is greater than the exciton binding energy. Exciton dissociation by this mechanism is usually a very efficient process in organic cells^{29,30}. Slight increases in the band-edge offset can increase charge-transfer rates; however, this value must be kept in check to maintain a high V_{oc} ³¹. Likewise, a prudent selection of compatible acceptor energy levels must be made to avoid losses in V_{oc} when employing low E_{gap} materials. Low E_{gap} materials, together with low-lying LUMO levels, appear to be the route to higher efficiency organic solar cells³².

The role of energy transfer in D/A heterojunctions has recently received considerable attention^{11,12,33,34}. As mentioned previously, in

addition to exciton diffusion to the D/A interface, some portion of the excitons may transfer their energy to the smaller E_{gap} material prior to exciton dissociation. If this two-step process is more efficient than D/A electron transfer, then the E_{gap} of the acceptor material must be smaller than that of the donor.

Phase separation

An ideal phase-separated network consists of a percolating and interpenetrating network of D/A phases approximately 100 nm in thickness. A thicker network will absorb more light, however, it does so at the expense of an increase in series resistance. A phase-separation length scale matched to the semiconductor exciton diffusion length (1–10 nm)^{35,36} will enable all excitons to reach an interface within their lifetime. Such an architecture can be approached with ZnO nanorods as a (nonabsorbing) high-mobility acceptor material, which is then infiltrated with a polymeric semiconductor as the donor^{37,38}. Issues with inefficient charge transfer to the oxide and charge transport in the tightly confined polymer have yet to be solved. Imperfect, yet highly functional phase-separated networks are known to form in polymer/small molecule systems, and are the basis for the highest performance organic solar cells. The holy grail of the phase-separated network consists of alternating groups within block copolymers that, when cast from a single solution, spontaneously assemble into ordered D/A arrays. Much work has been carried out to this end, however, optimizing these structures to incorporate polymers that match other design requirements continues to be challenging synthetically^{39,40}.

Photoactive organic materials

Polymeric donors

Presently, the polymer/fullerene materials system has emerged as a performance leader for solution-processed cells, with power conversion efficiencies^{41–43} that approach 5%. Current progress in polymeric donor materials has been outlined in several reviews^{36,44–46}. Device modeling suggests that by slightly tuning the LUMO levels of the polymer/fullerene system, efficiencies as high as 8.5% are within reach, and with increased layer thickness and balanced h^+/e^- mobility, 10.8% is the maximum efficiency predicted for polythiophene donors and fullerene acceptors³². In the near-term, an engineering solution exploits the semitransparency of OPV cells to increase efficiency. By stacking cells in tandem to increase photovoltage, no additional understanding of device physics has been necessary to surpass the 6% benchmark^{47–49}.

One area in need of further study in the current highest performance materials system, poly(3-hexylthiophene) (P3HT): [6,6]-phenyl C_{61} butyric acid methyl ester (**PCBM**) (compounds in bold are shown in Figs. 2 and 3), is in the characterization of the composition within phase-separated domains⁵⁰. High-resolution spectroscopy of the lateral chemical composition reveals that devices are typically composed of P3HT-rich domains that contain some equilibrium concentration of **PCBM**^{51,52}. Outside of these domains, the

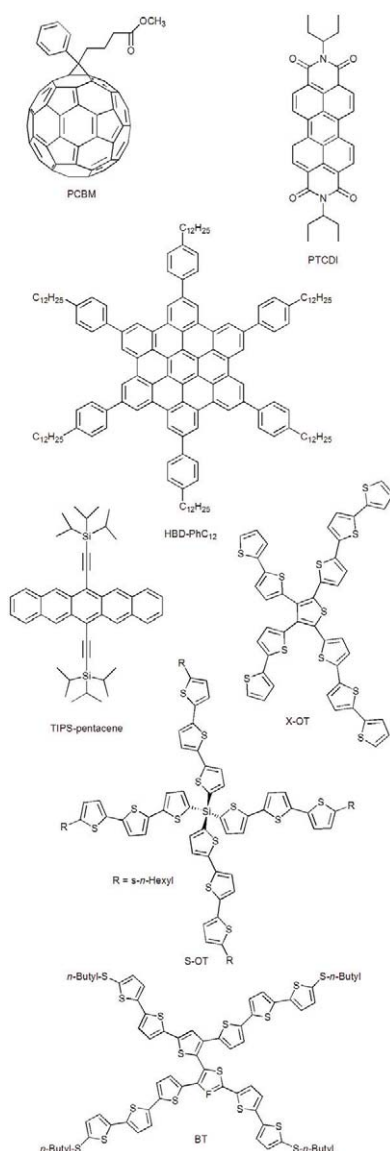


Fig. 2 Soluble acceptor and donor compounds.

concentration changes gradually to almost pure **PCBM**. This makes the optimal blending ratio difficult to identify, and a method to control composition uniformity over a large area has yet to be demonstrated.

Vapor-deposited small molecules

In addition to the advantages afforded by small molecules, such as high purity and ease of synthesis, vacuum sublimation makes small molecules the favored material for the study of fundamental photophysical processes. Vapor deposition permits sequential stacking of well-defined layers, easy calculation of the optical field profile^{53,54}, and extraction of exciton diffusion lengths^{25,55}. Bulk heterojunctions are also possible in small molecules via thermal vacuum co-deposition^{56–58}. The extent of phase separation can be controlled by managing the substrate temperature during deposition⁵⁷,

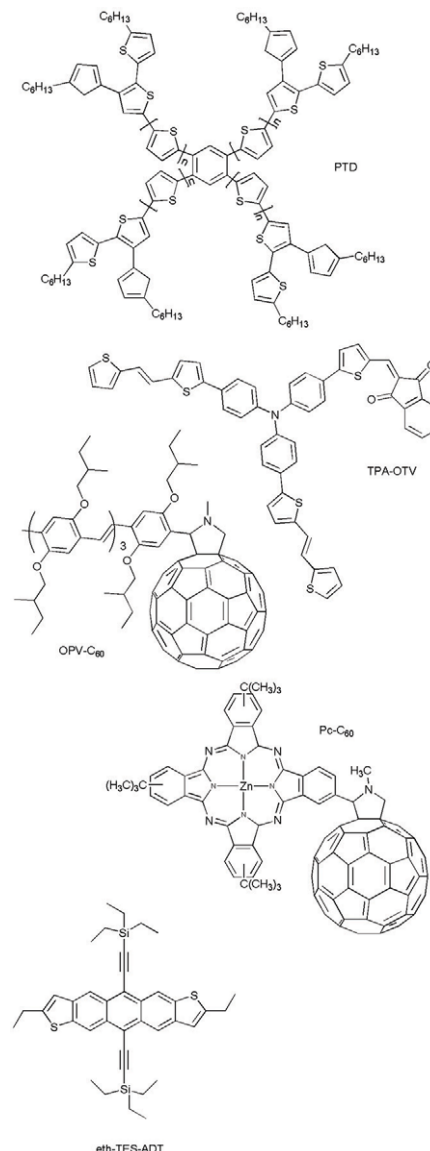


Fig. 3 Soluble conjugated D/A dyads and donor compounds.

post-fabrication thermal annealing⁵⁸, or solvent vapor annealing^{27,59}. Compared to bulk heterojunctions, layered heterojunctions are thought to limit the exciton generation volume. However, highly efficient cells (5–6%) have been made in layered heterojunction architectures^{48,60–62}. A thorough review of vapor-deposited small molecules has been recently published by Peumans *et al.*⁵⁴.

Soluble small molecules

Compared with polymeric semiconducting materials and vapor-deposited small molecules, soluble small molecules are commonly believed to be difficult to process⁶³ and have received comparatively little attention in the literature. Strong intermolecular forces between these conjugated small molecules facilitate intermolecular electron delocalization, which is desirable for efficient charge transport.

Unfortunately, these strong interactions are also responsible for the nucleation of molecular crystals in solution, which in many cases, results in poor film formation. That being said, many low molecular weight compounds have excellent film-forming capabilities with low surface roughness⁶⁴, morphologies that can be controlled with post-deposition treatments^{63,65}, and can be zone-purified *in situ*⁶⁶.

The following sections outline soluble small molecules whose performance as donor materials has been evaluated for use in OPV. There has been comparatively little exploration of soluble *n*-type molecules because of a scarcity of highly electron-deficient, air-stable conjugated molecules and the satisfactory performance of **PCBM** and *N,N'*-dimethyl-3,4,9,10-perylenetetracarboxyldiimides (**PTCDI**)^{45,67,68}.

Liquid crystals

The first application of soluble small molecules for photovoltaics in the form of liquid crystals was carried out by Schmidt-Mende *et al.*⁶⁹ in 2001. This cell used a functionalized hexabenzocoronene (**HBD-PhC₁₂**) discotic liquid crystal as the donor material, and a soluble perylene diimide (**PTCDI**) derivative as the acceptor. The donor material self-organizes into an array of nanoscopic columns that is interspersed with the acceptor phase. These devices can be fabricated by simple spin-coating techniques and produce external quantum efficiencies as high as 34% for low-intensity monochromatic (490 nm) light. Higher light intensity, however, causes rapid degradation, and performance at one-sun illumination intensity has not been reported.

Pentacene derivatives

Pentacene is perhaps the most ubiquitous of the small-molecule organic semiconductors. With a mobility that rivals that of amorphous Si⁷⁰ and reasonable air stability⁷¹, pentacene is a common choice for the transport layer in thin-film transistors (TFTs). Recently in the Anthony group^{72,73}, we have investigated pentacene derivatives such as 6,13-bis(triisopropylsilyl)ethynylpentacene (**TIPS-pentacene**). Unsubstituted pentacene adopts a herringbone motif in the solid state. This aromatic edge-to-face interaction can be disrupted by adding silyl substituents to the central ring of the pentacene molecule, leading to close cofacial π -stacking⁷². The TIPS side groups carry the additional advantage of imparting solubility and facile film formation to the insoluble pentacene molecule. **TIPS-pentacene** can be crystallized in the thin-film form, giving rise to a strong bathochromic shift, which indicates strong π -interactions. Since crystalline thin films absorb farther into the red than unsubstituted pentacene, in theory, this should lead to higher photocurrents and power conversion efficiency.

Unfortunately, when in solution, **TIPS-pentacene** rapidly undergoes a Diels-Alder reaction with fullerene derivatives⁷⁴. The result is a TIPS-pentacene-PCBM adduct with energy levels that ineffectively support photoinduced charge transfer. In a bilayer configuration with vacuum-deposited C₆₀, however, where adduct formation can be kept to a minimum, a photovoltaic response can be measured. After optimization

of layer thicknesses, incorporation of exciton-blocking layers, and thermal annealing, power conversion efficiencies reached a peak value of 0.5%⁷⁵. The modest performance can be attributed to restricted D/A elementary charge transfer. Despite a LUMO-LUMO offset greater than 1 eV and the broad absorption spectrum of **TIPS-pentacene**, measurements of the external quantum efficiency for these bilayers indicate that a majority of the photocurrent is generated in the blue end of the spectrum, where absorption originates from C₆₀.

Oligothiophenes

Sun *et al.*⁷⁶ have employed tetrasubstituted thienyl precursors in the synthesis of novel 'X'-shaped oligothiophene (**X-OT**) electron donors. Four compounds were synthesized in which the length of the four thiophene branches was systematically varied. The photovoltaic performance increases by two orders of magnitude between the smallest compound with three thiophene rings per molecule, and the largest compound with 11. This dramatic change is attributed to the film-forming capability, which is superior for the larger molecules, and broader absorption spectrum, which increases with the extent of π -conjugation. The best donor (**X-OT** in Fig. 2) produces a comparatively high short-circuit current (3.65 mA/cm²) and V_{oc} (850 mV), but a low fill factor (0.25) results in a power conversion efficiency of 0.8% with 100 mW/cm² illumination.

In an effort to enhance the processability of oligothiophenes, higher solubility has been attained by the synthesis of so-called swivel cruciform oligothiophenes dimers⁷⁷. This 'twisted' bi-thiophene (**BT**) shows a well-ordered structure in the solid state and relatively high TFT mobility (0.012 cm²/V.s) when deposited from a chloroform solution. More recently, Karpe *et al.*⁷⁸ reported the photovoltaic performance of **BT** in a bulk heterojunction with **PCBM**. Despite poor rectification behavior and a fill factor (0.27) that suggests high recombination rates, the devices show a power conversion efficiency of 0.2%.

Kopidakis *et al.*⁷⁹ have investigated the viability of phenyl-cored thiophene dendrimers (**PTD**) as a donor with **PCBM**. Although three-armed dendrimers have superior mobility, a four-armed dendrimer enables solution-cast film formation and ultimately yields a smaller optical E_{gap} . Atomic force microscopy (AFM) indicates that these solution-cast blends phase separate on a length scale < 10 nm. The authors suggest that high interface area in exceptionally fine blending reduces the fill factor (0.4 in these devices) by increasing recombination rates. Reducing the device thickness to 100 nm is found to increase the photocurrent (3.4 mA/cm²) and photovoltage (940 mV) to yield a spectrally corrected power conversion efficiency of 1.3% under AM1.5 (sunlight transmitted through 1.5 atmospheres) illumination, which is the highest soluble small molecule efficiency to date.

An issue with many OPV systems is that of molecular and crystal orientation. High anisotropy in light absorption and charge transport are important concerns for the future of solution-processed materials. A group at the University of Angers^{80,81} has sought to overcome the

low dimensionality of planar small molecules via synthesis of star-shaped oligothiophenes (**S-OT**) with a tetrahedral Si core. Absorption spectra of these compounds are identical in the thin-film and solution state, indicating an absence of aggregation or intermolecular π -interactions in the solid state. Within a bulk heterojunction, these molecules are likely to form amorphous hole-transporting networks that may inhibit charge collection. Power conversion efficiency in these devices is 0.3%, a relatively high value considering the transport limitations and the 440 nm light absorption onset.

Triphenylamines

Roquet *et al.*⁸² have investigated another route to three-dimensional conjugated molecules. Triphenylamine (**TPA**) derivatives are understood to have a high degree of non-coplanarity. Appending linearly conjugated oligothiophenevinylene (**OTV**) groups to **TPA** yields solid-state amorphous three-dimensional networks with isotropic optical and electronic properties. Adding electron-withdrawing groups to these derivatives lowers the oxidation potential for increased V_{oc} and decreases the optical E_{gap} for enhanced absorption. In a solution-processed bulk heterojunction with **PCBM**, this molecule leads to a simulated AM1.5 efficiency of 0.8%.

Anthradithiophene

Soluble triethylsilylthynyl-anthradithiophene (**TES-ADT**) molecules show high hole mobility in transistors and are subject to significant morphological reorganization upon exposure to solvent vapor⁶⁵. In bulk heterojunctions, Lloyd *et al.*⁸³ have found the photovoltaic performance of this material to depend critically on a solvent annealing treatment. As fabricated, the morphology of **ethyl-TES-ADT:PCBM** blends is amorphous with intimate donor-acceptor mixing that

quenches all photoluminescence. Upon exposure to solvent vapor, highly crystalline circular domains nucleate and grow. Reminiscent of spherulites in polymeric thin-films, these domains display a Maltese cross signature under crossed polarized light (Fig. 4a), indicating a long-range radial ordering of the crystallites. X-ray diffraction and AFM indicate that within the spherulites, submicron crystallites of **ethyl-TES-ADT** are dispersed in an amorphous matrix of **PCBM**. Measurements of the fractional spherulite coverage show a direct relationship between this morphological signature and both short-circuit current and device efficiency. Fabrication of a device with high spherulite coverage leads to a power conversion efficiency of 1% under illumination of 100 mW/cm².

Incomplete photoluminescence quenching (Fig. 4b) indicates that there are exciton decay pathways within the **ethyl-TES-ADT** crystallites other than charge transfer. With better understanding and control of solvent-induced crystal growth, a refinement of the crystallite size should lead to higher device efficiencies.

Donor/acceptor dyads

Although exciton dissociation processes in bulk heterojunctions have been shown to be extremely efficient by photoluminescence quenching⁵⁸ and time-resolved photoinduced absorption measurements⁸, the length scale of the phase-separated network and exciton diffusion lengths are still critical to obtain high device performance. To this end, a parallel effort in solution-processed small molecules has emerged where a single covalent bond controls the separation distance between discrete D/A molecules. The linked pair comprise a larger compound known as a dyad. In theory, all photons absorbed by thin-films of D/A dyads should be dissociated with very high yield independent of exciton diffusion behavior. In device design,

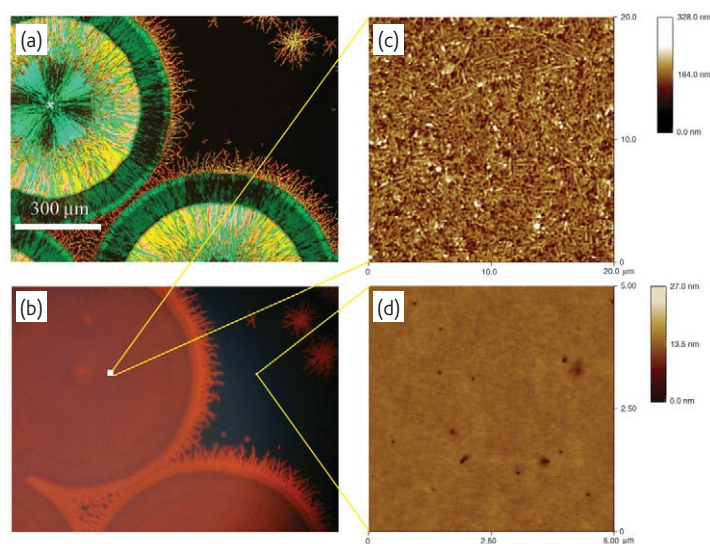


Fig. 4 (a) Crossed-polarized images of solvent-induced spherulite formation within an otherwise amorphous films of **ethyl-TES-ADT:PCBM**. (b) Photoluminescence of **ethyl-TES-ADT** is apparent within the spherulite, the intimate blending outside the spherulite completely quenches donor emission. (c) Highly crystalline interior of the spherulite. (d) The film is featureless with no evidence of phase separation outside the spherulite.

the challenge lies in charge extraction, where the dyads must organize to form percolating networks of D/A materials between the electrodes.

Oligo(p-phenylenevinylene)-fullerene (**OPV-C₆₀**) dyads show D/A charge transfer in thin films followed by long-lived charge separated states (~1 ms)^{11,84}. Peeters *et al.*¹¹ and Nierengarten *et al.*⁸⁵ have also measured unoptimized photovoltaic performance in solution-cast devices of these dyads. Later work by Neugebauer *et al.*⁸⁶ has characterized a Zn-phthalocyanine-fullerene (**Pc-C₆₀**) dyad. While the performance of these devices measures less than blends of discrete D/A small molecules, the observation of a photovoltaic response indicates that it is possible to form a phase-separated network of bound D/A pairs. Improvement in the design of the dyads should increase in the material absorption coefficient and a shift of the D/A molecular ratio closer to that found in higher performance polymer/fullerene cells.

Summary

While the power conversion efficiency of solution-processed small molecules has reached only modest values so far, research is still in its early stages. In terms of next-generation materials that are likely to increase present day efficiencies, two donor molecules stand out in particular. Synthetically uncomplicated **TIPS-pentacene**, with a thin-film absorption spectrum that extends to 700 nm, has demonstrated band-like transport and hole mobilities > 1 cm²/V.s in solution-cast TFTs^{87,88}. As mentioned earlier, in order to exploit these desirable traits, novel acceptor species are required to avoid chemical reactions with fullerenes. Another likely candidate, CuPc has demonstrated excellent photovoltaic performance in bilayer devices. The absorption spectrum of CuPc spans 550–750 nm, and lifetime studies carried out on TFTs point toward high environmental stability^{88,89}. Soluble analogues of this molecule are commercially available, yet there has been scarcely any research on its solution-processed photovoltaic performance.

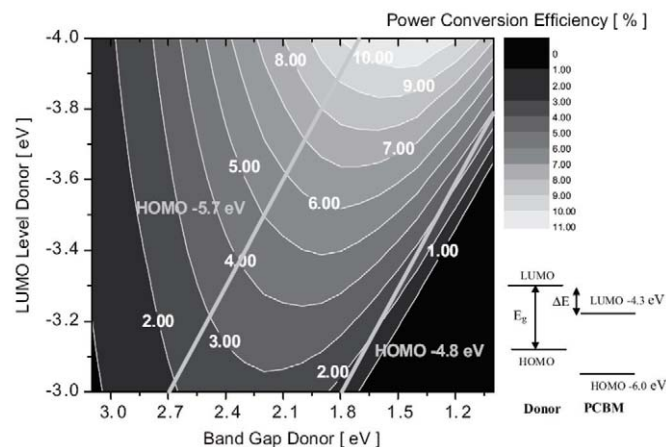


Fig. 5 Power conversion efficiency as a function of LUMO level and bandgap for the donor compound. The calculation assumes PCBM is the acceptor and that the external quantum efficiency and fill factor are maintained at 65%. (Reproduced with permission from⁹⁰. © 2006 Wiley-VCH.)

Perhaps the most exciting development on the horizon is shown in Fig. 5. Scharber *et al.*⁹⁰ calculate that efficiencies up to 10% are possible via energy-level tuning of the donor materials for devices using **PCBM** as the acceptor. By increasing the electron affinity and reducing the optical E_{gap} , it is possible to enhance absorption of the solar spectrum and maximize the theoretical V_{oc} . In the Anthony group, we recently synthesized anthradithiophene derivatives with LUMO levels approaching 4 eV. Fig. 6 compares the energy levels of

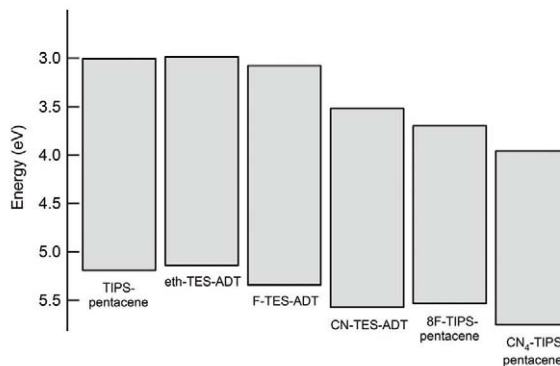


Fig. 6 Energy level diagram for soluble donors as measured by cyclic voltammetry.

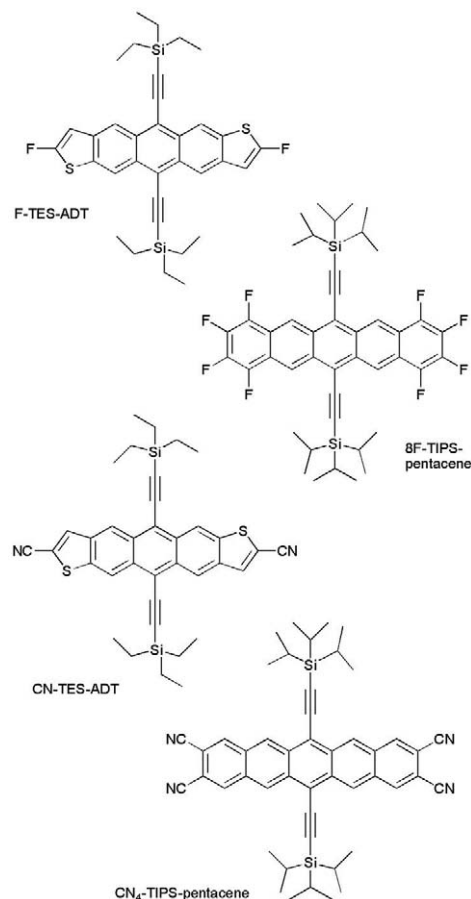



Fig. 7 Soluble acene donor compounds.

TIPS-pentacene and **ethyl-TES-ADT** with those of the larger electron affinity molecules **F-TES-ADT**, **CN-TES-ADT**, **8F-TIPS-pentacene**, and **CN₄-TIPS-pentacene** (Fig. 7). By optimizing solvent choice and controlling solvent evaporation rates, it should be possible to nucleate and grow crystalline domains on the order of an exciton diffusion length in such donor compounds. By tailoring energy levels and

employing common purification methods, calculated power conversion efficiencies should be well within the reach of these inexpensive, easily processable materials. 

Acknowledgments

The authors would like to thank the Office of Naval Research for continued financial support.

REFERENCES

1. Tang, C. W., *Appl. Phys. Lett.* (1986) **48**, 183
2. Gregg, B. A., *MRS Bull.* (2005) **30**, 20
3. Halls, J. J. M., et al., *Nature* (1995) **376**, 498
4. Yu, G., et al., *Science* (1995) **270**, 1789
5. Sundar, V. C., et al., *Science* (2004) **303**, 1644
6. Farchioni, R., et al., *Organic Electronic Materials: Conjugated Polymers and Low Molecular Weight Organic Solids*, Springer, New York, 2001
7. Hill, I. G., et al., *Chem. Phys. Lett.* (2000) **327**, 181
8. Sariciftci, N. S., et al., *Science* (1992) **258**, 1474
9. Brabec, C. J., et al., *Chem. Phys. Lett.* (2001) **340**, 232
10. Lee, C. H., et al., *Phys. Rev. B* (1993) **48**, 15425
11. Peeters, E., et al., *J. Phys. Chem. B* (2000) **104**, 10174
12. Liu, Y. X., et al., *J. Appl. Phys.* (2006) **99**, 093521
13. Kahn, A., et al., *J. Polym. Sci.: Polym. Phys.* (2003) **41**, 2529
14. Mühlbacher, D., et al., *Adv. Mater.* (2006) **18**, 2884
15. Shockley, W., et al., *J. Appl. Phys.* (1961) **32**, 510
16. King, R. R., et al., *Appl. Phys. Lett.* (2007) **90**, 183516
17. Wang, X., et al., *Adv. Funct. Mater.* (2005) **15**, 1665
18. Bundgaard, E., and Krebs, F. C., *Sol. Energy Mater. Sol. Cells* (2007) **91**, 954
19. Roncali, J., *Chem. Rev.* (1997) **97**, 173
20. Dhanabalan, A., et al., *Adv. Funct. Mater.* (2001) **11**, 255
21. Salzman, R. F., et al., *Org. Electron.* (2005) **6**, 242
22. Mandoc, M. M., et al., *Appl. Phys. Lett.* (2007) **90**, 133504
23. Koster, L. J. A., et al., *Appl. Phys. Lett.* (2006) **88**, 052104
24. Peumans, P., et al., *Chem. Phys. Lett.* (2004) **398**, 27
25. Terao, Y., et al., *Appl. Phys. Lett.* (2007) **90**, 103515
26. Markov, D. E., et al., *Phys. Rev. B* (2005) **72**, 045217
27. Gregg, B. A., *J. Phys. Chem.* (1996) **100**, 852
28. Karl, N., et al., *J. Vac. Sci. Technol. A* (1999) **17**, 2318
29. Xue, J. G., et al., *Adv. Mater.* (2005) **17**, 66
30. Brabec, C. J., et al., *Adv. Funct. Mater.* (2001) **11**, 15
31. Rand, B. P., et al., *Phys. Rev. B* (2007) **75**, 115327
32. Koster, L. J. A., et al., *Appl. Phys. Lett.* (2006) **88**, 093511
33. Hukka, T. I., et al., *Adv. Mater.* (2006) **18**, 1301
34. Lloyd, M. T., et al., unpublished results
35. Halls, J. J. M., et al., *Appl. Phys. Lett.* (1996) **68**, 3120
36. Blom, P. W. M., et al., *Adv. Mater.* (2007) **19**, 1551
37. Olson, D. C., et al., *Thin Solid Films* (2006) **496**, 26
38. Ravirajan, P., et al., *J. Phys. Chem. B* (2006) **110**, 7635
39. Hadziioannou, G., *MRS Bull.* (2002) **27**, 456
40. Sommer, M., et al., *Adv. Funct. Mater.* (2007) **17**, 1493
41. Ma, W., et al., *Adv. Funct. Mater.* (2005) **15**, 1617
42. Li, G., et al., *Nat. Mater.* (2005) **4**, 864
43. Kim, Y., et al., *Nat. Mater.* (2006) **5**, 197
44. Koeppe, R., et al., *Photochem. Photobiol. Sci.* (2006) **5**, 1122
45. Hoppe, H., et al., *J. Mater. Chem.* (2006) **16**, 45
46. Gunes, S., et al., *Chem. Rev.* (2007) **107**, 1324
47. Hadipour, A., et al., *Adv. Funct. Mater.* (2006) **16**, 1897
48. Xue, J. G., et al., *Appl. Phys. Lett.* (2004) **85**, 5757
49. Kim, J. Y., et al., *Science* (2007) **317**, 222
50. Yang, X., and Loos, J., *Macromolecules* (2007) **40**, 1353
51. McNeill, C. R., et al., *Small* (2006) **2**, 1432
52. van Duren, J. K. J., et al., *Adv. Funct. Mater.* (2004) **14**, 425
53. Pettersson, L. A. A., et al., *J. Appl. Phys.* (1999) **86**, 487
54. Peumans, P., et al., *J. Appl. Phys.* (2003) **93**, 3693
55. Yoo, S., et al., *Appl. Phys. Lett.* (2004) **85**, 5427
56. Gebeyehu, D., et al., *Sol. Energy Mater. Sol. Cells* (2003) **79**, 81
57. Geens, W., et al., *Thin Solid Films* (2002) **403**, 438
58. Peumans, P., et al., *Nature* (2003) **425**, 158
59. Conboy, J. C., et al., *J. Phys. Chem. B* (1998) **102**, 4516
60. Xue, J. G., et al., *Appl. Phys. Lett.* (2004) **84**, 3013
61. Chan, M. Y., et al., *Appl. Phys. Lett.* (2007) **90**, 023504
62. Forrest, S. R., *MRS Bull.* (2005) **30**, 28
63. Stingelin-Stutzmann, N., et al., *Nat. Mater.* (2005) **4**, 601
64. Bernards, D. A., et al., *Appl. Phys. Lett.* (2004) **84**, 3675
65. Dickey, C. D., et al., *Adv. Mater.* (2005) **18**, 1721
66. Liu, C. Y., et al., *Chem. Mater.* (2000) **12**, 2353
67. Hummelen, J. C., et al., *J. Org. Chem.* (1995) **60**, 532
68. Struijk, C. W., et al., *J. Am. Chem. Soc.* (2000) **122**, 11057
69. Schmidt-Mende, L., et al., *Science* (2001) **293**, 1119
70. Dimitrakopoulos, C. D., et al., *Adv. Mater.* (2002) **14**, 99
71. Facchetti, A., *Materials Today* (2007) **10** (3), 28
72. Anthony, J. E., et al., *Org. Lett.* (2002) **4**, 15
73. Anthony, J. E., et al., *J. Am. Chem. Soc.* (2001) **123**, 9482
74. Miller, G. P., et al., *Org. Lett.* (2003) **5**, 4199
75. Lloyd, M. T., et al., *Org. Electron.* (2006) **7**, 243
76. Sun, X. B., et al., *J. Phys. Chem. B* (2006) **110**, 7702
77. Zen, A., et al., *J. Am. Chem. Soc.* (2006) **128**, 3914
78. Karpe, S., et al., *Adv. Funct. Mater.* (2007) **17**, 1163
79. Kopidakis, N., et al., *Appl. Phys. Lett.* (2006) **89**, 103524
80. Roncali, J., et al., *Thin Solid Films* (2006) **511**, 567
81. Roquet, S., et al., *J. Mater. Chem.* (2006) **16**, 3040
82. Roquet, S., et al., *J. Am. Chem. Soc.* (2006) **128**, 3459
83. Lloyd, M. T., et al., *J. Am. Chem. Soc.* (2007), in press
84. van Hal, P. A., et al., *J. Phys. Chem. A* (2000) **104**, 5974
85. Nierengarten, J. F., et al., *Chem. Commun.* (1999) **7**, 617
86. Neugebauer, H., et al., *Sol. Energy Mater. Sol. Cells* (2004) **83**, 201
87. Ostroverkhova, O., et al., *Phys. Rev. B* (2005) **71**, 035204
88. Park, S. K., et al., *Appl. Phys. Lett.* (2007) **91**, 063514
89. Yan, X. J., et al., *Thin Solid Films* (2006) **515**, 2655
90. Scharber, M. C., et al., *Adv. Mater.* (2006) **18**, 789